

Controlled vibrational quenching of nuclear wave packets in D_2^+

Thomas Niederhausen* and Uwe Thumm†

James R. Macdonald Laboratory, Kansas State University, Manhattan, Kansas 66506-2604, USA

(Received 9 February 2007; revised manuscript received 2 October 2007; published 22 January 2008)

Ionization of neutral D_2 molecules by a short and intense pump laser pulse may create a vibrational wave packet on the lowest ($1s\sigma_g^+$) adiabatic potential curve of the D_2^+ molecular ion. We investigate the possibility of manipulating the bound motion, dissociation, and vibrational-state composition of D_2^+ nuclear wave packets with ultrashort, intense, near infrared control laser pulses. We show numerically that a single control pulse with an appropriate time delay can quench the vibrational state distribution of the nuclear wave packet by increasing the contribution of a selected stationary vibrational state of D_2^+ to more than 50%. We also demonstrate that a second control pulse with a carefully adjusted delay can further squeeze the vibrational-state distribution, thereby suggesting a multipulse control protocol for preparing almost stationary excited nuclear wave functions. The subsequent fragmentation of the molecular ion with a probe pulse provides a tool for assessing the degree at which the nuclear motion in small molecules can be controlled.

DOI: [10.1103/PhysRevA.77.013407](https://doi.org/10.1103/PhysRevA.77.013407)

PACS number(s): 42.50.Md, 33.20.Tp, 82.37.Np

INTRODUCTION

Enabled by significant advances in the technology of generating ultrashort and intense laser pulses over the past two decades, the nuclear dynamics in molecules has become observable in the time-domain [1–5]. In particular, the motion of vibrational and rotational wave packets in small diatomic molecules can be observed at a time scale of 10 fs and below, i.e., at and below the molecules' natural vibrational and rotational time scales [6–9].

In femtosecond pump-probe experiments [8,9], the fast ionization of neutral D_2 molecules in an intense fs pump laser pulse leads to the formation of molecular ions in a coherent superposition of excited rotational and vibrational states, i.e., to a moving nuclear (ro-) vibrational wave packet. Once launched, these wave packets propagate in the lowest $1s\sigma_g^+$ adiabatic potential curve of the molecular ion. The anharmonicity of this potential curve entails the rapid dephasing of the initial wave packet's vibrational state components within a few vibrational periods $T_{D_2^+} \approx 24$ fs of the molecular ion [8]. This leads to the eventual collapse of the nuclear wave packet, which has been predicted theoretically [10] and recently confirmed experimentally [8,9]. This collapse is—many vibrational periods later—followed by quarter (after ≈ 280 fs) and half revivals (after ≈ 560 fs) [11], indicating a localized periodic motion of the wave packet.

Going beyond the observation of the nuclear dynamics, possibly making an important contribution toward the overarching goal of achieving coherent control in chemical reactions [4,12], Niikura *et al.* [13,14] addressed the possibility of actively controlling the motion of vibrational wave packets by one additional short laser pulse. Using an intense “control” laser pulse that is long (18 fs) as compared to the present study, they investigated the controlled cooling, heating, and vibrational quenching into the vibrational ground state [13]. More recently, the same group measured a strong increase of the dissociation yield of D_2^+ by applying an 8 fs

control laser pulse when the vibrational wave packet is near its outer classical turning point [14]. In parallel to our investigation, Murphy *et al.* [15] have proposed a related control-pulse scheme for selecting stationary vibrational states of D_2^+ (in Franck-Condon approximation) and emphasize its possible use for quantum computing. In a slightly different approach Pe'er *et al.* [16] have used a femtosecond frequency comb in order to induce Raman transitions between vibrational levels of the Rb_2 molecule.

The idea of applying one (or several) control pulse(s) to a vibrational wave packet in the hydrogen molecular ion or its isotopes is the starting point for this investigation (Fig. 1). We will show that a control pulse that is appropriately delayed with respect to the pump pulse can modify the quantum dynamics of a nuclear wave packet by stimulating Raman transitions that alter the vibrational state composition of the wave packet in a controlled way, and that this control can be systematically improved by replacing a single control pulse with a carefully timed sequence of two (or more) short control pulses. In particular, we will show that through appropriate choice of the control pulse parameters (delay, duration, and peak intensity), a given lower excited stationary vibrational state can be selected. The quality of this Raman-control mechanism can be tested experimentally by fragmenting the molecular ion with an intense probe pulse and by identifying the nodal structure of the surviving vibrational state in the kinetic energy release spectrum of the molecular fragments. The combined population and probing of a specific vibrational state points to a possibility for imprinting and retaining information in the nuclear wave function using a three (or more) laser pulse setup.

THEORETICAL MODEL

Starting with neutral D_2 molecules in their vibrational (and electronic) ground state $\chi_{v=0}^{D_2}$, we first model the generation of the D_2^+ vibrational wave packet due to tunneling ionization of the neutral molecule in a 6 fs, 10^{14} W/cm², 800 nm pump-laser pulse. Because of the rapid increase of the molecular ionization rate with the internuclear distance R [17], the Franck-Condon (FC) approximation is not valid and

*esdimax@phys.ksu.edu

†thumm@phys.ksu.edu

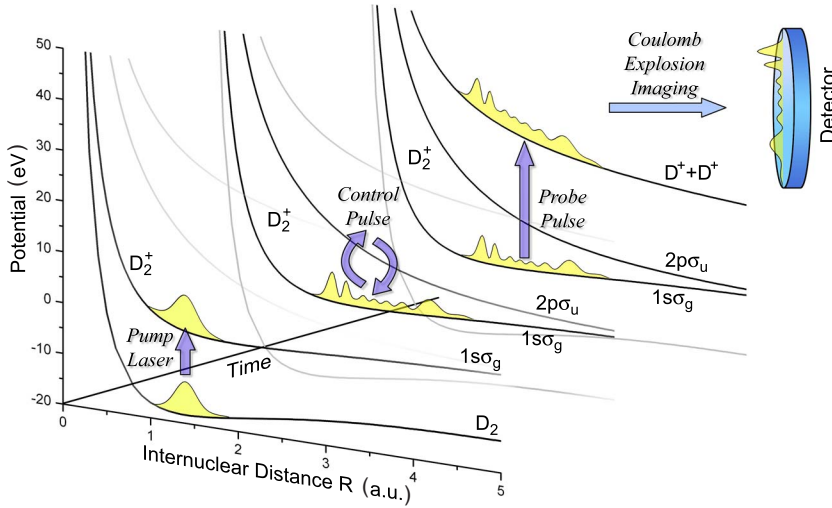


FIG. 1. (Color online) Schematic diagram showing the ionization of $D_2(v=0)$ by a pump pulse, followed by the modification of the vibrational wave packet on the $D_2^+ 1s\sigma_g^+$ potential curve by a control pulse, and the final destructive analysis through Coulomb explosion imaging by a probe pulse.

is known to generate a vibrational state distribution $\{\chi_\nu^{D_2^+}\}$ of the molecular ion that overestimates the population of higher excited vibrational states [18]. Specifically, we model the ionization of the neutral ground-state molecular ion in terms of the molecular Ammosov-Delone-Krainov (ADK) tunneling ionization rate $\Gamma_{\text{ADK}}^{D_2}(R, I)$ [19] that depends on the pump laser intensity I . This rate is based on the original rate for tunneling ionization of (one-electron) atoms in a static electric field [20] and owes its dependence on R to the implicit generalization of the atomic ionization potential to the vertical (at a given value of R) energy gap between the adiabatic energy of the neutral diatomic molecule [21] and its daughter molecular ion [22] in their respective ground electronic states. Even though $\Gamma_{\text{ADK}}^{D_2}(R, I)$ does not depend on the molecular orientation relative to the electric field \vec{E}_p of the pump laser, for single ionization of H_2 molecules that are perpendicularly oriented to \vec{E}_p , the isotropic rates lead to good agreement with the measured relative population of vibrational excited states in H_2^+ [18]. We note that for arbitrary orientation of the molecule relative to the laser electric field, orientation-dependent molecular ADK rates [23] would be more accurate. However, since the molecular orientation can be selected experimentally [3], for the purpose of our investigation, we disregard the orientation dependence of molecular ionization.

Since the initial eigenstate composition of the nuclear wave packet $\{\chi_\nu^{D_2^+}\}$ depends on the shape of the pump pulse, we assume in the following sections a 6 fs, 10^{14} W/cm² pulse launching the vibrational D_2^+ wave packet at time $t=0$, thereby starting the molecular clock [3]. Based on the depleted vibrational state of the D_2 molecule after the pump pulse,

$$\chi_{\text{pump}}^{D_2}(R) = \chi_{\nu=0}^{D_2}(R) \exp\left(-\int_{-\infty}^{\infty} \frac{\Gamma_{\text{ADK}}^{D_2}(R, I(t))}{2} dt\right), \quad (1)$$

we obtain the normalized initial wave packet in D_2^+ ,

$$\chi_{\text{initial}}^{D_2^+}(R, t=0) = \frac{\chi_{\nu=0}^{D_2} - \chi_{\text{pump}}^{D_2}}{\|\chi_{\nu=0}^{D_2} - \chi_{\text{pump}}^{D_2}\|}. \quad (2)$$

This approximation assumes instantaneous ionization, since we neglect the evolution of the nuclear wave function during

the ionization process. Indeed, for the considered 6 fs pump pulse, ionization occurs predominantly near the peak intensity of the laser electric field and can thus be considered as fast on the time scale of the nuclear motion. The $\chi_{\text{initial}}^{D_2^+}$ wave packet propagates on the $D_2^+ 1s\sigma_g^+$ potential curve and would undergo cycles of dephasing and revivals [8–10] without changing its vibrational states distribution $\{a_\nu = \langle \chi_\nu^{D_2^+} | \chi_{\text{initial}}^{D_2^+} \rangle\}$ if no further laser pulse would illuminate it. We will refer to this wave function as “ADK-wave packet.” However, the influence of one (or more) short and intense control pulses at variable delay times changes the shape of the wave packet by altering its vibrational amplitudes $\{a_\nu\}$ due to Raman transitions and dissociation (Fig. 1).

Allowing for Raman transitions between the two lowest adiabatic potential curves in D_2^+ , we adopt a two-state model for the propagation of the nuclear wave packet on the $1s\sigma_g$ and $2p\sigma_u$ potential curves (unless stated otherwise we will use atomic units),

$$i \frac{d}{dt} \begin{pmatrix} \chi_g \\ \chi_u \end{pmatrix} = (\hat{T} + \hat{V} + \hat{H}_c) \begin{pmatrix} \chi_g \\ \chi_u \end{pmatrix} \quad (3)$$

where the initial conditions for the nuclear wave packet components on the D_2^+ potential curves of gerade and ungerade symmetry are $\chi_g(R, t=0) = \chi_{\text{initial}}^{D_2^+}(R)$ and $\chi_u(R, t=0) = 0$, respectively. The kinetic energy operator $\hat{T} = p^2/(2\mu)$ includes the reduced mass $\mu = 1835$ of the two nuclei. The adiabatic electronic potential curves $1s\sigma_g$ and $2p\sigma_u$ of D_2^+ [22] form the diagonal elements of the potential

$$\hat{V} = \begin{pmatrix} V_g(R) & 0 \\ 0 & V_u(R) \end{pmatrix}. \quad (4)$$

The dipole coupling between the gerade and ungerade potential curves in D_2^+ , induced by one (or several) control pulses, is included in the off-diagonal elements of the coupling operator \hat{H}_c and depends on the electronic dipole moment between the two adiabatic electronic states (ψ_g and ψ_u) $d_{gu}(R) = \langle \psi_u | z | \psi_g \rangle$ [24] and the control laser electric field $E(t) = E_0(t) \sin \omega t$,

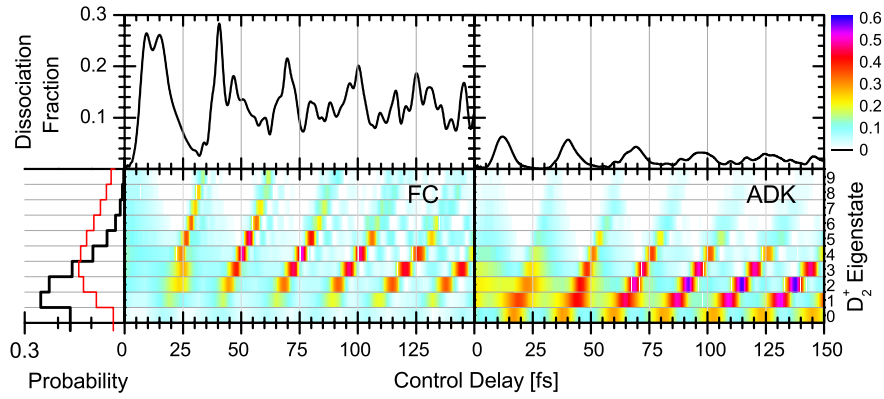


FIG. 2. (Color online) D_2^+ dissociation probability (top two graphs) and vibrational state distribution (bottom two graphs) after the control pulse as a function of the control pulse delay. The left two panels show the dissociation and state occupation assuming a Franck-Condon populated initial wave packet, while the right two panels correspond to the more realistic ADK initial-state distribution based on tunnel ionization of the neutral molecule. Both initial vibrational-state populations for D_2^+ after the pump pulse are shown on the left-side panel: for the ADK distribution using a 6 fs, 10^{14} W/cm 2 pump pulse (thick black line) and for the broadened distribution arising from a vertical Franck-Condon transition (thin red line). The control pulse is a 6 fs Gaussian pulse with an intensity of 10^{14} W/cm 2 .

$$\hat{H}_c = \begin{pmatrix} -\frac{i}{2}\Gamma_g^{D_2^+}(R) & d_{gu}(R)E \\ d_{gu}(R)E & -\frac{i}{2}\Gamma_u^{D_2^+}(R) \end{pmatrix}. \quad (5)$$

Not included in the present calculations are couplings beyond the Born-Oppenheimer approximation. In view of strong dipole couplings induced by an intense laser pulse, we expect nonadiabatic effects to be of little relevance for the present investigation [25].

Each control pulse has a Gaussian envelope

$$E_0(t) = E_{\max} \exp\left(-2 \ln 2 \frac{(t-t_D)^2}{w^2}\right) \quad (6)$$

centered at the control pulse delay t_D , with a full width at half maximum w and a laser peak intensity E_{\max}^2 . In the diagonal elements of \hat{H}_c we include the isotropic R -dependent molecular ADK rates for D_2^+ [19] in order to account for Coulomb explosion during the control pulse(s). The time propagation is carried out by solving the time-dependent Schrödinger equation (3) on a numerical grid, using the split-operator Crank-Nicholson scheme [26–28]. The numerical grid in R extends from 0.05 to 30 with a spacing of 0.05, and a time step $\Delta t=1$ for the nuclear motion is used. A quadratic optical potential

$$V_{\text{opt.}}(R) = -i\Theta(R-20)\left(\frac{R-20}{10}\right)^2 \quad (7)$$

with the Heavyside step function $\Theta(R)$ has been introduced at the outer grid end covering a width of 10 to avoid reflections.

The probability $P_\nu(t)=|a_\nu(t)|^2$ for finding the system at time $t>0$ in the ν th vibrational eigenstate is calculated as the quantum mechanical overlap of the bound wave function

$\chi_g(t)$ with the known field-free eigenfunctions $\chi_\nu^{D_2^+}(R)$ of the $1s\sigma_g$ potential curve (obtained by diagonalization of the Hamiltonian $\hat{T}+V_g$),

$$P_\nu(t) = \frac{|\langle \chi_\nu^{D_2^+} | \chi_g(t) \rangle|^2}{\langle \chi_g(t) | \chi_g(t) \rangle}. \quad (8)$$

By projecting onto field-free eigenfunctions, we simulate the vibrational distribution as it would be detected by an ideal probe pulse. Such a pulse induces instantaneous Coulomb explosion without prior distortion on its leading edge.

RESULTS

One control pulse

In our first numerical application, we consider a single (6 fs, 10^{14} W/cm 2) control pulse, and test the validity of the FC principle by comparing the results with the improved modeling (based on molecular ADK rates) of the initial wave packet generated by the pump pulse. The control pulse laser intensity is chosen such that a large fraction of the initial molecule remains bound. Compared with $T_{D_2^+}$, this pulse is short and leads to a nearly instantaneous transition between different electronic states.

Figure 2 shows the final vibrational state distribution (8) as a function of the control pulse delay for both the FC populated initial state and the ADK wave packet in D_2^+ . Due to the strong increase of the molecular ADK ionization rate $\Gamma_{\text{ADK}}^{D_2^+}(R,I)$ with the internuclear distance in D_2 , the vibrational-state distribution of the ADK-wave packet is narrower and shifted toward lower vibrational eigenstates, i.e., colder than the initial FC distribution [18]. The figure shows in both cases that after certain delay times the vibrational wave packet has largely collapsed to one single vibrational level. It is evident that the control-pulse-delay times at which population maxima appear in a certain vibrational state $\chi_\nu^{D_2^+}$

is identical for both initial-state distributions, although the maxima strongly differ in amplitude. The control-pulse delay times at which the relative contribution of a stationary vibrational state $\chi_\nu^{D_2^+}$ is most prominently enhanced is related to the classical period T_ν for the motion of a particle (of mass μ) on the binding potential curve V_g with the energy E_ν of the vibrational state $\chi_\nu^{D_2^+}$,

$$T_\nu = 2 \int_{R_{\min}}^{R_{\max}} dR \sqrt{\frac{\mu}{2[E_\nu - V_g(R)]}}, \quad (9)$$

where R_{\min} and R_{\max} are the classical turning points. However, since the center of the initial wave function $\chi_{\text{initial}}^{D_2^+}(R)$ is created outside the inner turning point, the delay times \tilde{T}_ν at which the first relative population surge of a given stationary vibrational state contribution occurs are shifted to slightly smaller delays ($\tilde{T}_\nu < T_\nu$). Due to the anharmonicity of the potential, and consistent with the increase of T_ν with ν , the time-delay difference between population surges of different vibrational-state contributions increases with increasing ν .

Caused by the rapid increase of the dipole coupling $d_{gu}(R)$ with R , the dissociation yield is largest near the outer turning point and negligible near the inner turning point (top two graphs in Fig. 2). For a few vibrational periods, the dissociation yield oscillates with the vibrational period of the molecular ion with maxima in the dissociation probability appearing at identical times for both initial-state populations. However, as the wave packet dephases [10,11], the oscillations decrease in amplitude and become increasingly smeared out. In addition, Fig. 2 shows that the total dissociation probability is generally larger for the FC model, since the larger contribution of higher-lying vibrational states tends to enhance dissociation in the laser pulse.

We now focus on the vibrational-control scheme for an initial vibrational ADK-wave packet arising from R -dependent tunnel ionization of the neutral molecule with a pump laser of 10^{14} W/cm² intensity. Figure 3 (top panel) shows the time evolution of the wave packet's probability density without a control pulse. Without additional laser interactions, the wave function starts to quickly dephase due to different phase accumulations of its stationary vibrational-states components. The center of the nuclear wave packet (superimposed curves in Fig. 3, computed as the expectation value for R) becomes stationary at $\langle R \rangle \approx 2.6$ after a propagation time of approximately 80 fs. Deviations from this equilibrium distance (not shown) only occur many vibrational cycles later due to wave-packet revivals [8–11]. The two particular control-delay times of 91.7 fs (Fig. 3, middle panel) and 96.3 fs (bottom panel) equal $4T_{\nu=2}$ and $4T_{\nu=3}$ for the second and third excited vibrational state, respectively. As seen in Fig. 2, a control pulse applied at delay times that equal a multiple of the oscillation period (9) of a particular state, strongly enhances the population of that state. At the chosen delay times for the control pulse at an intensity of 10^{14} W/cm², optimal enhancement of the vibrational occupation for the $\nu=2$ and $\nu=3$ state is obtained, with $P_2(t_D=91.7 \text{ fs})=55.1\%$ and $P_3(t_D=96.3 \text{ fs})=49.9\%$, respectively. Also seen in the top panel of Fig. 2 is that more than 97% of

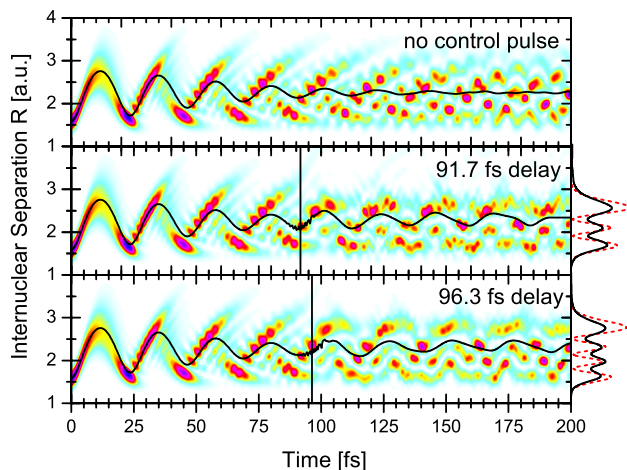


FIG. 3. (Color online) Time evolution of a nuclear ADK-wave packet probability density without the presence of a control pulse (top) and with a control pulse at a delay of 91.7 fs (middle) or 96.3 fs (bottom). The solid line represents the center of the bound wave packet $\langle R \rangle$. The two vertical lines indicate the control-pulse delays. The dashed red line in the side panel shows the known nodal structure for the second and third excited vibrational state, respectively, while the solid black line is the average of the wave-packet probability density over the 100 fs directly following the control pulse. The intensities of pump and control pulse are 10^{14} W/cm².

the molecular ion remains bound at these two control-pulse-delay times.

If the control pulse completely quenches the wave packet into a single vibrational eigenstate, its probability density would be stationary and display the nodal structure of that state in terms of horizontal “stripes” in Fig. 3 (middle and bottom panel). This nodal structure could be imaged by further ionizing the molecular ion in a sudden vertical transition onto the repulsive $D^+ + D^+$ potential curve with an intense and short probe pulse. This technique of mapping nuclear probability densities onto the kinetic energy release spectrum of the emitted fragments is well-established and commonly referred to as laser-induced “Coulomb-explosion imaging” [3,6–8,14]. It is thus possible, with existing technology, to quantify the extent to which the nuclear wave packet can be compressed. In the present examples, the dominant population of the second or third excited vibrational state contributions explains the emergence of the nodal structure of these states as wavy horizontal light blue lines with small amplitudes in the middle and bottom panel of Fig. 3, respectively. The dominant stationary vibrational state can more clearly be identified in the time average over the 100 fs immediately after the control pulse (side panels of Fig. 3): minima and maxima appear at the same positions as for the stationary $\chi_2^{D_2^+}$ and $\chi_3^{D_2^+}$ wave functions. Further refinement of this selection can be achieved by adjusting the shape of the control pulse or by applying several control pulses. This would tend to more distinctly display wave function nodes in the kinetic-energy-release spectrum.

The ripples near the control-delay time in the expectation value $\langle R \rangle$ in Fig. 3 appear due to the Rabi oscillations between the gerade and ungerade potential curves and indicate

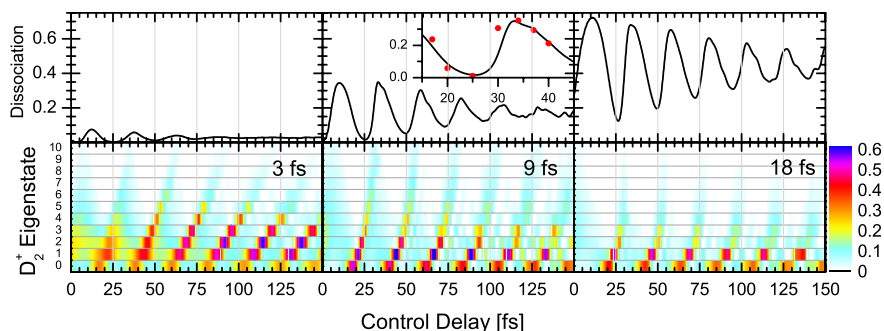


FIG. 4. (Color online) Dissociation probability (top) and final-state population (bottom) for an ADK-wave packet as a function of the control-pulse delay, shown for a near single-cycle 3 fs pulse (left), an intermediate pulse length of 9 fs (middle), and a relatively long control pulse of 18 fs (right). The pump-pulse intensity is 10^{14} W/cm 2 and the control-pulse intensity 2×10^{14} W/cm 2 . For comparison, the inset shows the measured dissociation yield by Niikura [14], scaled to our calculated results.

the physical mechanism behind the controlled change of the vibrational wave packet: successive Raman transitions between vibrational states on the $1s\sigma_g$ potential curve, mediated through dipole transitions between the two lowest adiabatic electronic states of D_2^+ .

Control pulse shape dependence

The influence of the control-pulse length on the vibrational-state-selective population is shown in Fig. 4 for a control-laser intensity of 2×10^{14} W/cm 2 . Clearly seen is that the temporal dependence remains unchanged with maxima in the population appearing according to Eq. (9). Except for the lowest vibrational state, the magnitude of these maxima suggests an optimal control-pulse length that is significantly shorter than $T_{D_2^+}$. This agrees with the fact that the longest control-pulse length (18 fs) renders the picture of a stationary nuclear wave function during the laser interaction invalid, and the spatial distribution broadens when the control-pulse length approaches the natural oscillation period of the molecular ion $T_{D_2^+}$. On the other hand, we find that the control pulse length does not significantly change the population of the ground vibrational state in accordance with the results in Ref. [13]. Our results agree qualitatively with [13] for the spatial position of the first maximum in the ground-state occupation at $t_D=20$ fs, but

the lack of an initial-state distribution does not allow for a direct comparison.

In addition, the longer control pulse and hence the higher energy transfer to the molecule induces stronger dissociation. For the 9 fs control pulse in Fig. 4 (top center panel), our calculated dissociation probability is in very good agreement with the measurement of Niikura *et al.* [14] (see inset) and agrees with their calculations.

For a short 6 fs control pulse, the laser intensity dependence is shown in Fig. 5. Above 2×10^{14} W/cm 2 , dissociation due to evaporation of the higher-lying vibrational states becomes significant and oscillates strongly with the vibrational period of the molecule [14], thus leading to vibrational cooling. The lowest vibrational eigenstates are therefore best accessed by applying a more intense control pulse, while higher excited states require a lower control-laser intensity. The temporal position of the maximum-state population remains unaffected by the control-laser intensity and only depends on the control-pulse delay time (cf. Fig. 2). Hence the varying control-pulse intensity within the laser focus, and deviations from the Gaussian envelope of the pulse are not expected to compromise the possibility of precisely quenching the vibrational motion into a particular state by carefully adjusting the control-pulse-delay time. For practical purposes, Table I provides a few examples of optimal control pulse parameters (delay time, peak intensity) found in this study for populating a particular low-lying vibrational state.

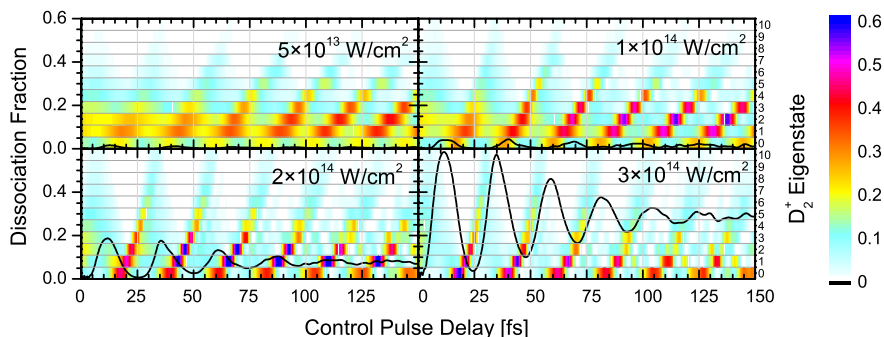


FIG. 5. (Color online) Combined dissociation probabilities (black curves) and final state populations for four different control-pulse intensities shown inside the graphs at fixed control pulse lengths of 6 fs. The pump pulse intensity is 10^{14} W/cm 2 .

TABLE I. Optimized parameters of the control pulse (intensity and delay t_D) for quenching a nuclear wave packet in the ground state or one of the first five excited states ν . The initial state populations P_ν^{initial} correspond to a 6 fs, 10^{14} W/cm² pump pulse. The final state probabilities P_ν^{final} and dissociation probabilities are obtained long after t_D . P_ν^{initial} , P_ν^{final} , and the dissociation yield are given in percent. The control-pulse intensity is given in 10^{14} W/cm² for an 800 nm control pulse.

ν	Intensity	t_D (fs)	P_ν^{initial}	P_ν^{final}	Dissociation
0	3	18.4	16.29	59.8	24.1
0	3	40.2	16.29	53.1	34.6
1	2	43.2	25.17	60.5	7.32
1	2	65.8	25.17	64.2	8.90
2	2	46.4	22.64	61.3	4.06
2	1.5	69.2	22.64	63.1	3.10
3	1.5	48.6	15.78	49.8	1.71
3	1	72.4	15.78	46.7	2.08
4	1.5	51.2	9.526	37.2	1.19
4	1	76.0	9.526	36.3	0.67
5	1.5	27.6	5.242	20.4	0.023
5	1	53.6	5.242	23.1	0.004

Two control pulses

In an attempt to further control the “slowing down” of the vibrational wave packet and with the ultimate goal in mind of “stopping” [13] it into a given stationary vibrational state, we now investigate the action of two control pulses. Both control pulses are 6 fs long with a peak intensity of 10^{14} W/cm². A scheme for enhancing a particular lower vibrational state is demonstrated for the $\nu=2$ state. For the first control pulse an optimal delay time was found at 70.7 fs. It produces a nuclear wave packet with a maximum combined population in the $\chi_2^{\text{D}_2^+}$ and $\chi_3^{\text{D}_2^+}$ vibrational states (Fig. 6). This delay time is intermediate between $3T_2=68.8$ fs and $3T_3=72.2$ fs. The delay of the second control pulse with respect to the center of the first control pulse was varied and a strong enhancement of the $\nu=2$ vibrational-state contribution was found at a delay time of 66.1 fs $\approx 3T_2$, when the second control pulse vibrationally cools the wave packet, mainly from the $\chi_3^{\text{D}_2^+}$ to the $\chi_2^{\text{D}_2^+}$ state. The underlying Raman transitions in the evolution of the vibrational states in Fig. 6 are indicated by the rapid oscillations of $\langle R \rangle$ near the control-pulse delay times. For this sequence of control pulses the bound vibrational wave packet of the molecular ions owes 77.3% to the stationary $\nu=2$ state, while the total dissociation yield is below 3%. This is in contrast to a previously proposed control scheme [13] that simulates nearly complete vibrational cooling into the $\nu=0$ vibrational ground state at a much higher dissociative loss.

SUMMARY AND OUTLOOK

In conclusion, we find in this numerical study that a short and intense control pulse can significantly alter the

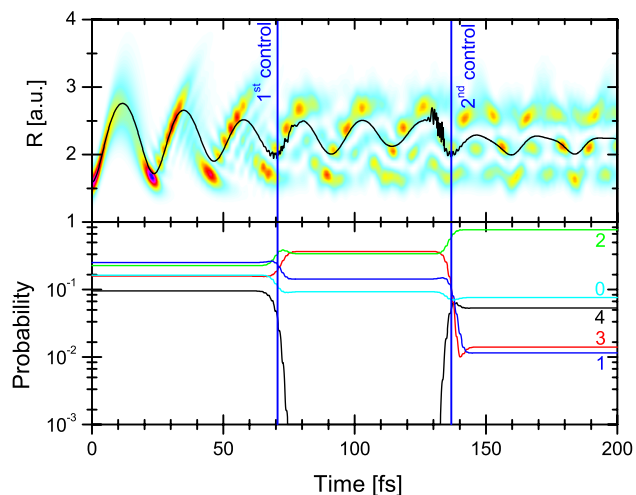


FIG. 6. (Color online) Time evolution of the ADK wave packet probability density (top) and the few lowest vibrational states (bottom, logarithmic scale) for two 6 fs, 10^{14} W/cm² control pulses with delay times of $t_1=70.7$ fs and $t_2=136.8$ fs relative to the start of the wave packet. The superimposed curve in the top graph shows the center motion $\langle R \rangle$ of the bound wave packet. The pump-pulse intensity is 10^{14} W/cm².

vibrational-state composition of nuclear wave packets in D_2^+ by coherent Raman transitions. A detailed understanding of exactly how the Raman sequence affects the final vibrational-state distribution $\{a_\nu\}$ and how the final $\{a_\nu\}$ depends on the control-laser parameters (pulse-length, intensity, shape, control delay) remains a challenge and will be addressed in a future publication. For the particular parameters in our model calculations we find that a single control pulse can populate a particular stationary vibrational state of D_2^+ with more than 60% probability, and that this fraction can be further increased by adding control pulses at appropriate delays that are given by integer multiples of the classical vibrational periods. The possibility of extending this multicontrol-pulse scheme to pulse trains [16] is evident and might enable the coherent control of dynamical processes in molecular systems. Preparing a quantum system in a particular state with the help of precisely timed control laser pulses can possibly be applied to store information in an almost stationary nuclear wave function and to retrieve the eigenstate information from the nodal structure at a later time by the interaction with a probe pulse.

ACKNOWLEDGMENTS

We thank J. McKenna for stimulating discussions. This work was supported by the NSF (Grant No. PHY-0354840) and the Division of Chemical Sciences, Office of Basic Energy Sciences, Office of Energy Research, and U.S. DOE.

- [1] J. H. Posthumus, Rep. Prog. Phys. **67**, 623 (2004).
- [2] A. Stolow, A. E. Bragg, and D. M. Neumark, Chem. Rev. **104**, 1719 (2004).
- [3] A. S. Alnaser, X. M. Tong, T. Osipov, S. Voss, C. M. Mahajan, P. Ranitovic, B. Ulrich, B. Shan, Z. Chang, C. D. Lin, and C. L. Cocke, Phys. Rev. Lett. **93**, 183202 (2004).
- [4] I. V. Hertel and W. Radloff, Rep. Prog. Phys. **69**, 1897 (2006).
- [5] C. D. Lin, X. M. Tong, and T. Morishita, J. Phys. B **39**, S419 (2006).
- [6] H. Stapelfeldt, E. Constant, H. Sakai, and P. B. Corkum, Phys. Rev. A **58**, 426 (1998).
- [7] I. V. Litvinyuk, K. F. Lee, P. W. Dooley, D. M. Rayner, D. M. Villeneuve, and P. B. Corkum, Phys. Rev. Lett. **90**, 233003 (2003).
- [8] T. Ergler, A. Rudenko, B. Feuerstein, K. Zrost, C. D. Schröter, R. Moshhammer, and J. Ullrich, Phys. Rev. Lett. **97**, 193001 (2006).
- [9] A. Rudenko, T. Ergler, B. Feuerstein, K. Zrost, C. D. Schröter, R. Moshhammer, and J. Ullrich, Chem. Phys. **329**, 193 (2006).
- [10] B. Feuerstein and U. Thumm, Phys. Rev. A **67**, 063408 (2003).
- [11] R. W. Robinett, Phys. Rep. **392**, 1 (2004).
- [12] T. Brixner, G. Krampert, T. Pfeifer, R. Selle, G. Gerber, M. Wollenhaupt, O. Graefe, C. Horn, D. Liese, and T. Baumert, Phys. Rev. Lett. **92**, 208301 (2004).
- [13] H. Niikura, D. M. Villeneuve, and P. B. Corkum, Phys. Rev. Lett. **92**, 133002 (2004).
- [14] H. Niikura, D. M. Villeneuve, and P. B. Corkum, Phys. Rev. A **73**, 021402(R) (2006).
- [15] D. S. Murphy, J. McKenna, C. R. Calvert, I. D. Williams, and J. F. McCann, New J. Phys. **9**, 260 (2007); J. McKenna (private communication).
- [16] A. Pe'er, E. A. Shapiro, M. C. Stowe, M. Shapiro, and J. Ye, Phys. Rev. Lett. **98**, 113004 (2007).
- [17] A. Saenz, J. Phys. B **33**, 4365 (2000).
- [18] X. Urbain, B. Fabre, V. M. Andrianarijaona, J. Jureta, J. H. Posthumus, A. Saenz, E. Baldit, and C. Cornaggia, Phys. Rev. Lett. **92**, 163004 (2004).
- [19] J. P. Brichta, W.-K. Liu, A. A. Zaidi, A. Trottier, and J. H. Sanderson, J. Phys. B **39**, 3769 (2006).
- [20] M. V. Ammosov, N. B. Delone, and V. P. Krainov, Zh. Eksp. Teor. Fiz. **91**, 2008 (1986) [M. V. Ammosov, N. B. Delone, and V. P. Krainov, Sov. Phys. JETP **64**, 1191 (1986)].
- [21] L. Wolniewicz, J. Chem. Phys. **99**, 1851 (1993).
- [22] D. R. Bates Kathleen Ledsham, and A. L. Stewart, Philos. Trans. R. Soc. London, Ser. A **246**, 215 (1953).
- [23] X. M. Tong, Z. X. Zhao, and C. D. Lin, Phys. Rev. A **66**, 033402 (2002).
- [24] K. C. Kulander, F. H. Mies, and K. J. Schafer, Phys. Rev. A **53**, 2562 (1996).
- [25] T. K. Kjeldsen and L. B. Madsen, Phys. Rev. Lett. **95**, 073004 (2005).
- [26] W. H. Press, B. P. Flannery, S. A. Teukolsky, and W. T. Vetterling, *Numerical Recipes* (Cambridge University Press, Cambridge, England, 1992).
- [27] U. Thumm, *Book of Invited Papers, XXII ICPEAC, Santa Fe, NM*, edited by S. Datz *et al.* (Rinton Press, Princeton, New Jersey, 2002), p. 592.
- [28] B. Feuerstein and U. Thumm, Phys. Rev. A **67**, 043405 (2003).